Thin Film Thickness Measurements in Two Phase Annular Flows using Ultrasonic Pulse Echo Techniques.

Y. A. Al-aufi[1], B. N. Hewakandamby[1], G. Dimitrakis[1], M. Holmes[2], A, Hasan[3] N. J. Watson[1] *

[1] Faculty of Engineering, University of Nottingham, University Park, Nottingham NG7 2RD, UK

[2] School of Food Science and Nutrition, University of Leeds, Woodhouse lane, Leeds LS29JT, UK

[3] Faculty of Science and Engineering, University of Hull, Cottingham road, Hull HU67RX, UK

* Corresponding Author.
Address: Dr Nicholas James Watson. Room B16, Coates Building, University Park, University of Nottingham, Nottingham, Nottinghamshire, NG7 2RD, UK.
Email: nicholas.watson@nottingham.ac.uk
Phone: (+44) 115 74 84848

Abstract:

The electric power generation and oil/gas production industries have a strong interest in the physical characterization of conducting and non-conducting liquid films that are formed during the flow of liquids in pipes. Conducting and non-conducting liquid films do not lend themselves to the same characterization techniques due to the different requirements originating from their electrical properties. Techniques based on the use of ultrasound are extremely attractive for that purpose as they do not depend on the electrical properties of the liquid and are also non-invasive. This paper presents the application of ultrasonic techniques for measuring the thickness of wavy thin liquid films (<6 mm) in vertical pipes. Initial benchtop experiments were performed, and different signal processing methods were implemented in order to identify the most suitable depending on the film thickness. For a film thickness >0.5 mm a time of flight method was utilized whereas for a film thicknesses <0.5 mm a frequency method and time domain method were utilized. These methods were validated using a theoretical volume measurement on a static system. The studied methods were then tested on downward and upward vertical flow experimental rigs with pipe diameters of 127mm and 34.5mm respectively. The results of the experiments using ultrasonic methods showed good agreement with the measurements obtained using a multi pin film sensor and a concentric conductance probe, highlighting the potential that ultrasound offers in thin film measurements.

Keywords: Thin Liquid Film Thickness, Ultrasonic measurements, Two-phase flow

36

37

1. Introduction:

Two phase flows (e.g. liquid and gas) are common in nature as well as in industrial applications [1]. Despite their importance they are still one of the least understood areas of fluid mechanics due to the complexities of the deforming interfaces and the dynamic dispersity of the phases within each other. However, models that apply to various flow regimes supported by system specific correlations based on measurements exist and are used in process and equipment design. The integrity of the data, therefore, is paramount to the success of the design and the predictability of the flow. Most of the correlations in use are developed using water as the liquid phase and steam or air as the gaseous phase in gas-liquid two phase flow systems. The universality of these correlations is yet to be proven as most seem to be system specific. For this particular reason, correlations, specifically the fitting constants, are generally established through measurements for various liquid flows where the physical properties are often different from water.

Annular flow is the most frequently observed two phase flow regime [2]. Risers in oil platforms, boiler tubes in power generation, and industrial condensors are all industrial examples that experience annular flow. In annular flow, the liquid flows partly as a thin film along the pipe wall and partly as droplets entrained in the turbulent gas core. The film is driven by the interfacial shear imparted by the gas flow and this coupling of momentum between the two phases leads to various interfacial behaviors [2]. While there are capillary waves propagating on the film, large coherent waves (in pipes with small diameters) travel on the film intermittently, at a much larger speed. These waves are often called disturbance or roll waves. Though intermittent, these waves seem to have somewhat regular periodicity for given liquid and gas flow rates [2, 3, 4]. The highly dynamic, complex interfacial phenomena, which are dependent on the gas and liquid flow rates and the physical properties of the two phases present one of the greatest challenges in developing theoretical models describing the hydrodynamics of the film [4]. However, capturing the characteristics of the liquid film is essential for the development of predictive models [1, 2] used for efficient and safe equipment design and operation. To this end, phenomenological models underpinned by the measurements of the local film thickness and flowrates should be developed. Local liquid film thickness measurements provide information to estimate the gas void fraction, hence the liquid and gas velocities [5]. Furthermore, such measurements provide means to test the existing correlations for their fidelity.

There has been substantial experimental research studying the behaviour of annular flow and readers can refer to the reviews of Azzopardi [3], Clark [6] and Berna et al. [7] for further details. The majority of previous work has focussed on liquid gas annular flow but two liquid annular flows have been studied and reviewed by Ghosh et al. [8]. The previous research has focussed on studying the annular thin film thickness and the features of the disturbance waves (frequency, amplitude/height and velocity). The features of the disturbance waves have received interest as they have significant effects on heat and mass transfer between the gas and liquid phases which is essential to understand, for industrial applications such as condensers and evaporators [9]. The measurement methods used to study the film and wave

74 features have been classified by Clark [6] as film averaged methods, localised methods and point methods.
75 Film average methods measure the volume of liquid in a section of pipe by isolating it using valves at
76 either end of the section under investigation. These techniques can be used to calculate average film
77 thicknesses but do not provide information on the characteristics of the disturbance waves. Localised and
78 point methods are more common in the literature as they can be used to determine spatial and temporal
79 characteristics of the liquid film and disturbance waves. Localised and point methods differ as localised
80 methods perform measurements over a defined spatial region whereas point methods perform
81 measurements at a single spatial location. Different sensors methods have been used to study film
82 thickness and disturbance waves including a variety of optical techniques [6,7, 10-15], conductance or
83 capacitance sensors techniques [16, 17], ultrasonic methods [18] or those that place tracer materials
84 (often radioactive) within the fluid [19]

85 Results from previous experimental work has shown that these different measurements can successfully
86 be used to characterise the film and disturbance wave features in annular flow. Zadrazil et al. [10] showed
87 that planar laser induced florescence measurements could be used to measure the frequency and
88 amplitude of disturbance waves in upward annular flow. Pham et al. 2016 [11] and Kunugi et al. [15}
89 showed that a high speed camera could be used to study the effect that spacers within a pipe section had
90 on disturbance waves. Pan et al. [13] used high speed photography in vertical upward gas liquid annular
91 flow to show that increases in gas velocity reduced the film thickness. Vasques et al. [9] studied upward
92 and downward gas/liquid annular flow and used measurements from a brightness based laser induced
93 florescence technique to demonstrate that the disturbance wave behaviour was dependent on flow
94 direction. Wang et al. [14] used Near-Infrared measurements at two points to study the velocity of
95 disturbance waves at different gas pressures in vertical upwards gas/liquid flow. Belt [17] used
96 conductance probes at 32 circumferential locations and 10 axial locations to study disturbance wave
97 features in upward gas liquid annular flow. Although the majority of work has focussed on the film and
98 wave features several researchers have studied the entrainment of liquid droplets into the gas core. For
99 more details on liquid entrainment the reader can refer to the review of Berna et al. [7]

100 Many of the liquid film measurement techniques have been developed using water as a liquid phase by
101 exploiting the advantage of its electrical properties (i.e high conductivity). These work are also often
102 performed in transparent pipes. Therefore, the developments of techniques that can operate with a non-
103 conducting medium such as oil and in systems with opaque pipe wall materials are required. In this
104 present study water and silicone oil were used as the liquid phases. Silicone oil was selected as its physical
105 properties resemble typical process liquids used in the oil and gas industry and is an electrically non-
106 conducting fluid. Water was also utilized so experimental results could be compared to those in the
107 literature which generally use water as the liquid phase.

108 In the present work, an ultrasonic pulse echo technique has been applied to measure the liquid film
109 thickness where the signal is transmitted and received by the same transducer. It is a non-intrusive
110 measurement technique that can easily be attached to different locations on the pipe and operates on
111 opaque materials such as PVC and metals. The ultrasonic pulse echo technique has been used by Chun et
112 al. [18] to investigate the effects of wall thickness, wall material, and ultrasonic frequency on liquid film
113 thickness measurements. They also compared the technique against theoretical calculations using static

films on plate and tube test sections. They concluded that the ultrasonic pulse echo technique can be used when the tube wall thickness ($\delta_{w,min}$) is greater than the value specified by:

$$\delta_{w,min} \geq Nc_w/2f \tag{1}$$

Where N is the number of wave cycles in the ultrasonic pulse, c_w is the speed of ultrasonic wave in the wall material and f is the frequency of ultrasonic wave. If the tube wall thickness is greater than this value the reflected waves are superimposed upon one another and signal and data analysis becomes challenging. This study also concluded that the acoustic impedance mismatch between the wall material and the liquid film should be low enough to allow the signals to be transmitted into the liquid film and the reflected signal from the liquid film/air interface distinguishable. Lu et al. [20] measured condensate film thickness using an ultrasonic pulse echo technique in a horizontal rectangular test section. They indicated that the ultrasonic measurements for wavy films could be improved by increasing the data acquisition rate (received waves/second). Serizawa et al. [21] evaluated ultrasonic measurements against a laser displacement gauge and impedance probe in stratified flow over a horizontal plate test section. They found an excellent agreement between the three measurement techniques. However, they indicated that the ultrasonic measurement has poor detection sensitivity due to the varying angle of the reflection interface. Chen et al. [22] used ultrasonic measurements to monitor the dynamic behavior of condensing and non-condensing fluid films. They proposed a new data processing method based on spectral analysis using a Fourier Transform to measure film thicknesses from 50 to 750 μm. Ultrasonic techniques have also been employed in two phase flow by many researchers to identify flow regimes [23-27]. However, most of the research was performed using ultrasonic techniques to measure liquid film thicknesses greater than 1mm and to identify the flow regimes on a horizontal pipe using air/water systems.

In the present study, the capability of the ultrasonic technique for measuring liquid film thicknesses in the range of 0.1 to 6 mm was examined for static films (in bench top experiments) as well as for dynamic films in annular flow within a cylindrical pipe. A Time of Flight (TOF) method was utilised for film thicknesses >0.5 mm, whereas time domain and frequency domain methods were used for film thicknesses <0.5 mm. The ultrasonic measurements were compared with a Multi Pin Film Sensor (MPFS) and a concentric conductance probe in both a downward and upward vertical flow rig using an air/water system, to assess its accuracy and applicability to dynamic films.
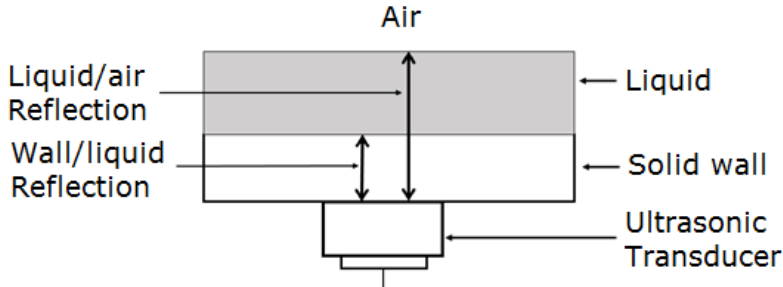
2. Principle of Ultrasonic Pulse Echo Techniques:

Ultrasonic techniques operate by transmitting low amplitude, high frequency acoustic waves through the system under investigation [28]. Ultrasonic pulse echo techniques can be used to calculate distances by measuring the time difference between transmitted and reflected pulses and knowledge of the speed of sound in the medium. This can be better demonstrated by studying a system consisting of three different layers as shown in Figure 1. These three layers are a solid wall, a liquid film and air. An ultrasonic transducer is attached to the solid wall. When an ultrasonic pulse is transmitted from the transducer, it will be partly reflected at the solid wall/liquid interface and received back by the same transducer as shown in Figure 1. The remaining acoustic energy will be transmitted through the liquid and then reflected back from the liquid film/air interface to also be received by the transducer. The Time of Flight (TOF) (Δt)

152 of the ultrasonic wave through the liquid film can be determined by recording the time difference
153 between the first reflected pulse at the solid wall/liquid film interface and the first reflected pulse at liquid
154 film/air interface (Figure 2). The liquid film thickness (δ) can then be calculated from the measurement of
155 the TOF using:

156 $\delta = C_L \Delta t / 2$ (2)

157 Where C_L is the ultrasonic wave speed of sound in the liquid phase.

158

159 Figure 1: Schematic of pulse echo technique showing the two reflections of the ultrasonic pulse in a
160 system consisting of three different layers (solid wall, liquid film and air).
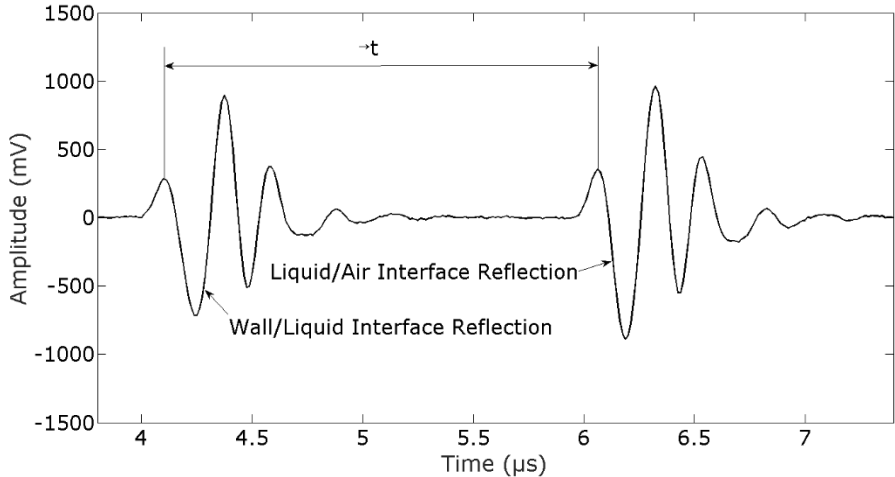
161

162 Figure 2: Ultrasonic reflected signals from wall/liquid and liquid/air interfaces showing the time
163 difference between them.

164 Care must be taken to ensure the correct reflected pulse is used for calculations. Acoustic reverberations
165 exist within the solid wall, but the liquid/air interface can be identified by varying the thickness of the
166 liquid layer. The TOF method can only be used when the two reflected signals do not overlap in time.
167 Therefore, the TOF is useful for films having a thickness greater than half the pulse wavelength, multiplied
168 by the number of cycles in the pulse. This is approximately 0.45 mm for a water film while using a 5 MHz
169 transducer with three cycles in the pulse.

170 For thin films (<0.5 mm) the reflected signal will become overlapped in time and alternative signal
171 processing strategies are required. There has been a variety of work in the literature using ultrasonic
172 methods to measure thin films with applications in lubricants (29, 30), Condensing films (22), adhesive
173 layers (31) and multilayer systems (32, 33). Numerous methods have been used to calculate the film or
174 layer thicknesses from the ultrasonic measurements including resonance methods (22, 29, 35), spring
175 models (29, 34, 35), wavelet analysis (36, 37), fractional Fourier Transforms (38) and matching pursuit
176 methods (31, 39). The proposed methods process the signals in the time or frequency domain or use a
177 method which is a combination of both. Time domain methods generally focusses on identifying the
178 individual reflections in the overlapped waves using deconvolution methods (40). Spring model methods
179 have been used extensively to measure thin films (~0.01-20 μm) between two solid materials by
180 calculating reflection coefficients as a function of frequency. The capability of the measurement system
181 depends on the frequency of the transducer utilised. The spring model also requires a reference signal
182 which is a reflection from an interface of known properties which is not always possible in some
183 experimental and real-life systems. The spring model can also be used for multilayer systems when
184 applying the Gaussian echo pre-processing steps suggested by (40).

185 The majority of previous work has been on a thin layer bounded by two stationary solid materials of known
186 properties. This is not the case for gas/liquid annular flow where the liquid is flowing and has a different
187 material of either side. An additional level of complexity is involved as the liquid/gas interface is in a
188 constant state of change with the presence of disturbance waves. In this work we will study two different
189 signal processing methods for thin films, one in the frequency domain and one in the time domain. The
190 frequency domain method will use the technique developed by Chen et al. [22] and the time domain
191 method will focus on the technique used by Park et al. [41]. These methods were selected as they have
192 been used previous on solid/liquid/gas systems which most closely represent the annular flow we will
193 study.

2.1 Frequency domain method:

195 For a thin film thickness less than 0.5mm, a frequency domain method developed by Chen et al. [22] can
196 be used. The thin liquid film (δ) can be calculated from:

197 $\delta = C_L/4f_0$ (3)

198 Where f_0 is the lowest frequency in the spectral data. As this cannot often be detected f_0 is taken as half
199 of the average interval distance between each pair of adjacent spectral peaks. The method of Chen et al.
200 [22] requires numerous signal processing steps to calculate f_0. First, a baseline signal is subtracted from
201 the received signals. This baseline is a signal recorded from a liquid film with infinite thickness. This
202 contains only a single reflection from the wall/liquid interface which is located at the same position for all
203 measurements made during the experiments. The remaining signal is then multiplied by a "flat top"
204 window function. This is performed by a point-by-point multiplication. The center half of the signal is
205 multiplied by one while both the beginning and end quarters were multiplied by coefficients which taper
206 from one at the center to zero at the ends. The flat top function is used to improve the signal to noise
207 ratio. The next step requires the signal to be zero padded to ensure it contains a number of samples which

208   is a power of two. This is performed to improve the efficiency of the following step which is to calculate
209   the Fast Fourier Transform (FFT) of the signal. The FFT creates a power density spectrum, and the
210   frequencies of the main spectral peaks are identified. The interval between each pair of adjacent spectral
211   peaks is calculated and all intervals in a given spectrum are averaged. The average interval is divided by
212   two to determine f_0, which is then used to calculate the layer thickness using Equation (3). An example of
213   an overlapped waveform signal (Figure 3a) and frequency spectrum after applying the frequency method
214   (Figure 3b) for a 0.2 mm liquid film thickness is shown in Figure 3. The three main frequency spectrum
215   peaks are identified at approximately 1.8, 4.1 and 6.4 MHz.
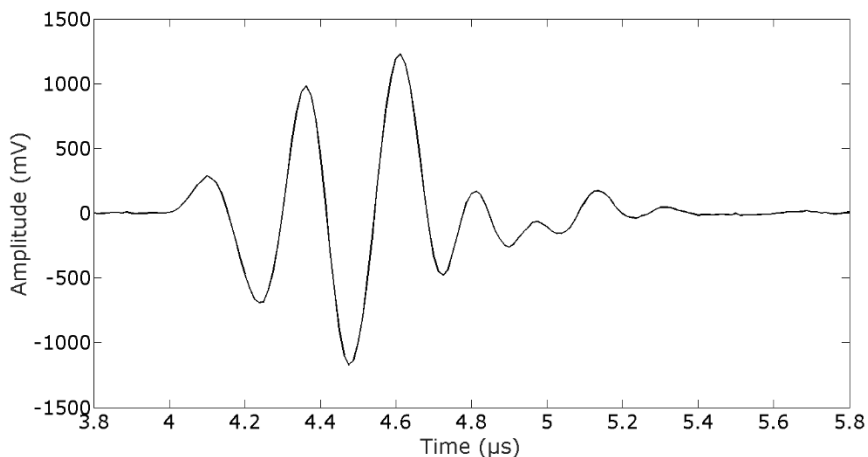
216

217   (a)
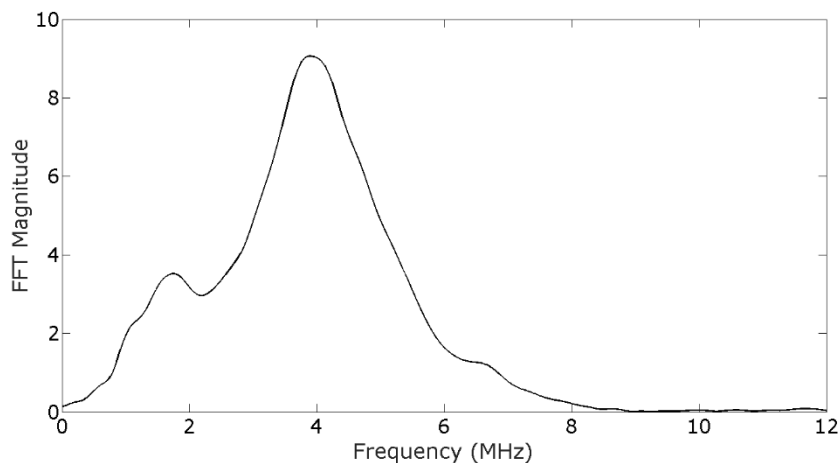
218

219   (b)

220   Figure 3: Original overlapped reflected waveform signal (a) and frequency spectrum after applying the
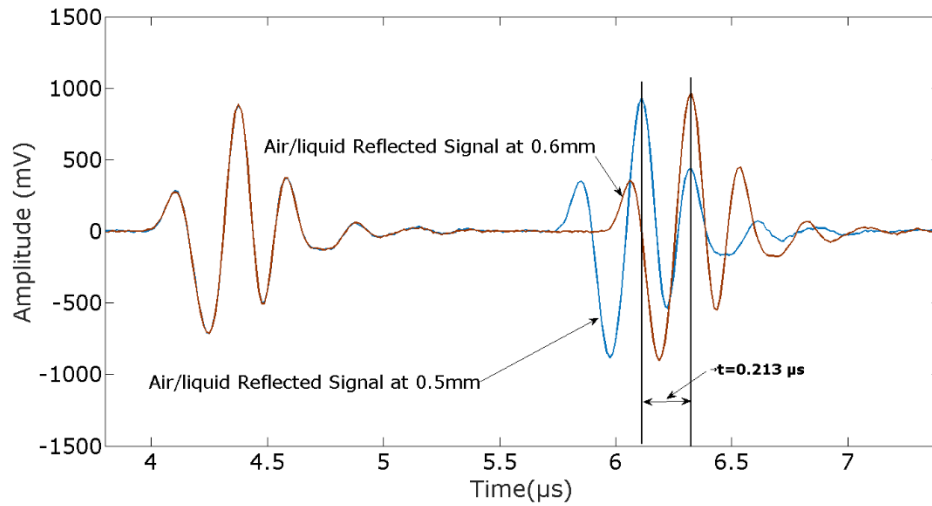221   frequency method (b) for a 0.2 mm liquid film thickness

222

223

2.2 Time Domain (Baseline removal) method:

The measurement of the film thickness using a TOF method (Equation 2) depends on identifying the first wall/liquid film reflected signal and the first liquid film/air reflected signal. When the liquid film is less than 0.5mm, the first liquid film/air reflected signal will overlap in time with the first wall/liquid film reflected signal (for a 5Mhz 3 cycle pulse). This makes the two reflected signals interfere with each other and results in a signal which includes components reflected from both interfaces. However, there is a time difference between the two reflected signals where the first wall/liquid film reflected signal will always arrive before the first liquid film/air reflected signal. Figure 4 displays a three layer system (wall/liquid film/air). The first wall/liquid film reflected signal arrives after the wave propagates through the wall and reflects from the wall/liquid interface. In contrast, the first liquid film/air reflected signal arrives after the wave propagates through the wall and the liquid film and reflects from the liquid film/air interface. Therefore, the difference between the two reflected signals is the time taken by the wave to propagate through the liquid film twice. As an example, if the minimum liquid film thickness (L) is 0.1mm, this means the time difference between the two reflected signals will be related to the time required for the wave to travel 0.2mm (2L). This can be demonstrated from the example given in Figure 5 which shows two reflected waves from different film thicknesses of silicone oil (0.5mm (blue line) and 0.6mm (orange line)). There is a 0.1mm difference of film thickness between the two waveforms and it can be observed that there is a time difference between the two signal's maximum amplitude by the approximate time interval of 2L which is equal to 0.213µs.
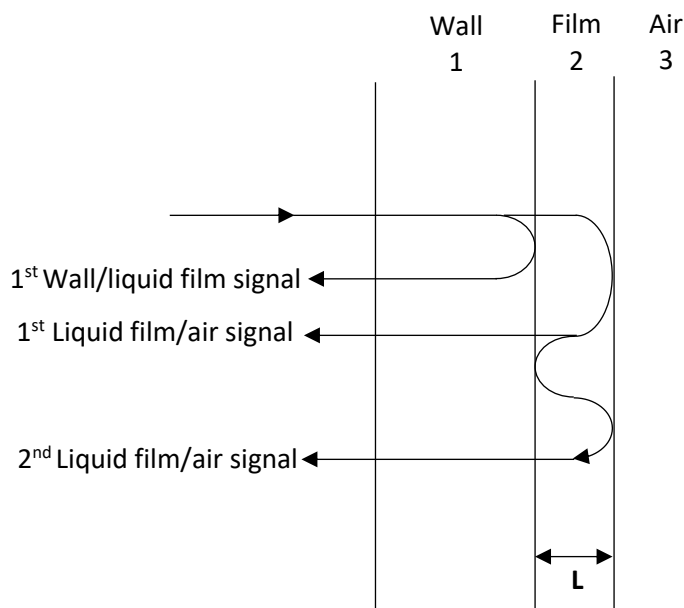
Figure 4: Diagram of the expected ultrasound wave paths for the three layers, a solid wall, a liquid film and air [17].

Figure 5: Two measurement waveforms with a 0.1 mm difference in film thickness. The first wall/film signal is identical for the both two measurement waveforms (0.5mm (blue line) and 0.6mm (orange line)).

The first reflected wall/liquid film reflected signal is always at the same location with the same amplitude for all measurements of different liquid film thicknesses, as the wall has constant geometric dimensions. This was confirmed by plotting received signals through wall/liquid film/air systems with varying liquid film thicknesses (Figure 5). However, for the signal reflected from the wall/liquid interface to remain in a constant location the wall and liquid temperature should not be varied during the experiments. In addition, the transducer position should be kept fixed and vibrations within the test section should be eliminated or minimised. To identify the location of the wall/liquid film signal without interference from other reflections a film of relatively large thickness (>1 cm) can be generated and the received signals recorded. This signal is then labelled as the baseline. Once this baseline signal has been recorded experiments can be performed with thin film thicknesses on unknown size. The baseline removal method operates by subtracting the baseline signal from the recorded signals with unknown film thicknesses. This results in three signals: the baseline signal, the unprocessed signal and the signal after subtracting the baseline (Figure 6). The TOF through the liquid film can then be calculated by subtracting the time of the first signal peak from the baseline signal from the first signal peak of the processed signal and applying Equation 2.

To demonstrate the baseline removal method, Figure 6 shows an example of the method for a silicone oil film thickness of 0.1 mm. In Figure 6, the amplitude of three signals is plotted in the same figure with respect to time. The three signals are the original unprocessed overlapped signal (Red line), baseline signal (Black line) and the processed signal after subtracting the baseline signal (Blue line). From Figure 6, it can be observed that the time difference between the two reflected signals is 0.213 μs which is the same as the value demonstrated in Figure 5.
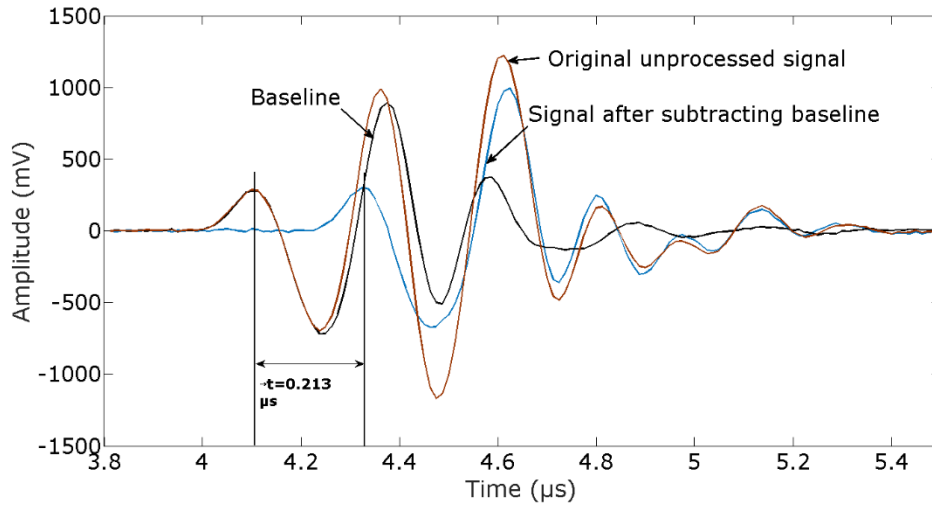
Figure 6: Ultrasound signals illustrating the baseline removal method for a film thickness of 0.1 mm. Original unprocessed signal (Red line), Baseline (Black line) and Signal after subtracting baseline (Blue line).

3. Experiment Setup:

The ultrasonic pulse-echo technique was validated using static and dynamic measurements. In the static measurements, the ultrasonic technique was validated using a benchtop experiment using water and silicone oil (4.4 cP) as the fluids. The ultrasonic technique was also validated against two other well-known measurement techniques based on conductance measurements using an air/water system under dynamic conditions. Each method of validation will be discussed in detail in the following subsections.

4.1. Static Measurement:

The ultrasonic technique was validated using silicone oil (4.4 cP) as shown in the schematic diagram in Figure 7. The validation was for static fluid conditions with film thicknesses between 0.1 mm and 6 mm. A cylindrical test section made of acrylic resin Perspex (Internal Diameter = 24.8 mm, wall thickness=5 mm and Height= 20 mm) was used. A Technisonic transducer model IPM-0502-HR 5MHz was used for these experiments. This was located in the centre of the bottom external surface of the test section. The diameter of the test section was measured using a digital caliper with an accuracy of +/-0.01 mm, and the volume was measured using a Gilson's Pipetman Classic with an accuracy of +/-2 µL. In the current study, a US-KEY (Lecoeur Electronique) was used as the transmitter, receiver and digitiser. The received signals were recorded and the film thicknesses calculated using bespoke MATLAB code based on the methodologies described above. The thickness of the film measured by the ultrasonic technique was compared with those calculated theoretically using:

$$\delta_{th} = V/A \tag{4}$$

Where δ_{th} is theoretical film thickness (mm), V is the volume (mm^3) and A is the cross-sectional area (mm^2).

10
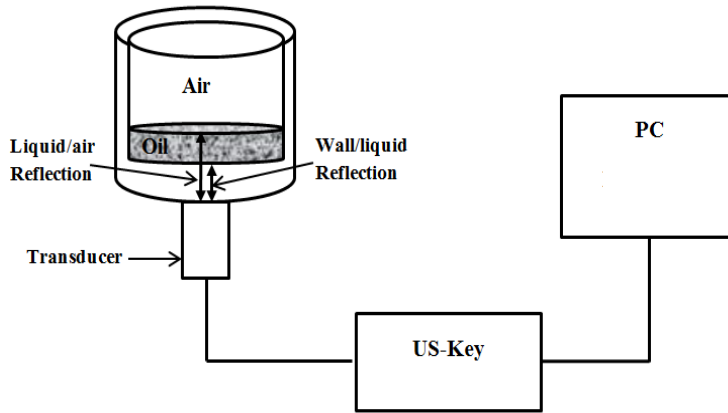
295

296   Figure 7: Schematic diagram of the static experiment using a cylindrical test section.

297   Silicone oil with 4.4 cP viscosity was used as it can generate film thicknesses less than 1 mm. It was difficult
298   to generate thin films less than 1 mm using water due to surface tension effects. The speed of sound of
299   the silicone oil at temperatures ranging between 10 and $45°C$ at atmospheric pressure was measured
300   using a TF instruments RESOSCAN as shown in Figure 8. These measurements were required to account
301   for any temperature effects on the sound propagation velocity during the experiments. The measurement
302   of silicone oil speed of sound was repeated three times during heating and cooling and the maximum
303   speed of sound coefficient of variation was within 0.02%. The coefficient of variation is defined as the
304   ratio of the standard deviation to the mean.

305   The speed of sound in silicone oil can be calculated using equation (5) based on repeated measurements
306   obtained using the TF instruments RESOSCAN.

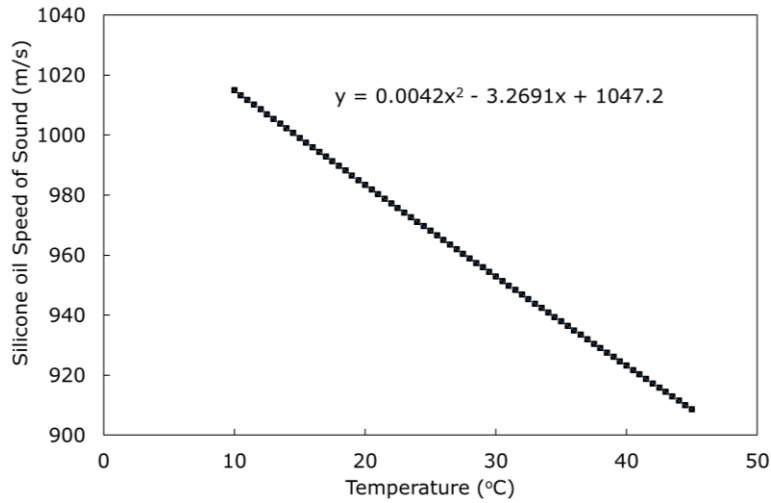307 $$C_l = 1.0472 \times 10^3 - 3.2691T + 4.2 \times 10^{-3}T^2 \qquad (5)$$

308   Where T is the temperature in degrees Celsius. This equation is valid for temperature range 10-45°C at
309   atmospheric pressure.

310

$$y = 0.0042x^2 - 3.2691x + 1047.2$$

311

Figure 8. Speed of sound of silicone oil (4.4cP) for a temperature range of 10-45°C at atmospheric pressure.

The RESOSCAN measurements were validated by measuring the speed of sound of distilled water for a temperature range of 10-45°C at atmospheric pressure and comparing with those available in the literature [42]. The results are shown in Figure 9. The relative deviation between RESOSCAN and Equation 6 was ±0.04%.

$$C_L = 1.40238677 \times 10^3 + 5.03798765T - 5.80980033 \times 10^{-2}T^2 + 3.34296650 \times 10^{-4}T^3 - 1.47936902 \times 10^{-6}T^4 + 3.14893508 \times 10^{-9}T^5 \tag{6}$$

Where *T* is the temperature in degrees Celsius. This equation is valid for a temperature range of 0-100°C at atmospheric pressure.
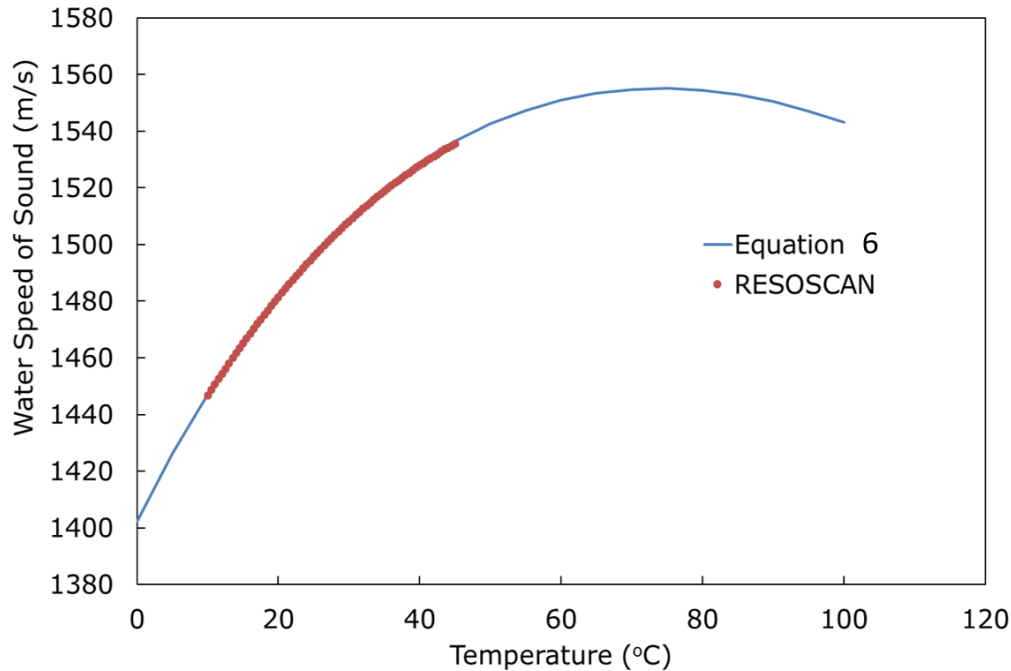
Figure 9: Comparison of speed of sound measurements in water using a RESOSCAN with literature (Equation 6).

Distilled water was also used to validate the film thickness measurements with a different test rig using a rectangular tank made of acrylic resin Perspex (width= 110 mm, length = 200 mm, wall thickness=5 mm and Height= 50 mm). The US-KEY and a Technisonic transducer model IPM-0102-HR 1MHz were used. The same method of validation with silicone oil was followed with distilled water. This was used to validate the ultrasonic technique for film thicknesses between 2 and 6 mm. This test rig is also capable of investigating the effect of inclination angle (incident wave angle) on measurement capability. Ultrasonic measurements are affected by reflections from interfaces which are not perpendicular to the incident wave. The further this angle is from the perpendicular the greater the effect on reflected wave detection sensitivity as the wave will be reflected away from the receiving transducer [21]. The angle was adjusted during experiments by lowering the test rig from one side. This angle was measured using a clinometer digital measurement. The other end of the test rig was fixed with a pivot joint so the test rig could be easily tilted. These experiments were performed on a film with a 6 mm thickness. The effect of inclination angle will be discussed in section 5.1.1.

4.2. Dynamic Measurements:

The capability of the ultrasonic pulse echo techniques to measure film thicknesses in a flowing test facilities was evaluated by comparing measurements with other established sensing technologies. A free falling liquid film annular flow test facility and an upward vertical annular flow test facility as shown in Figure 10 and Figure 11 respectively were used with water as the liquid phase.

13

344
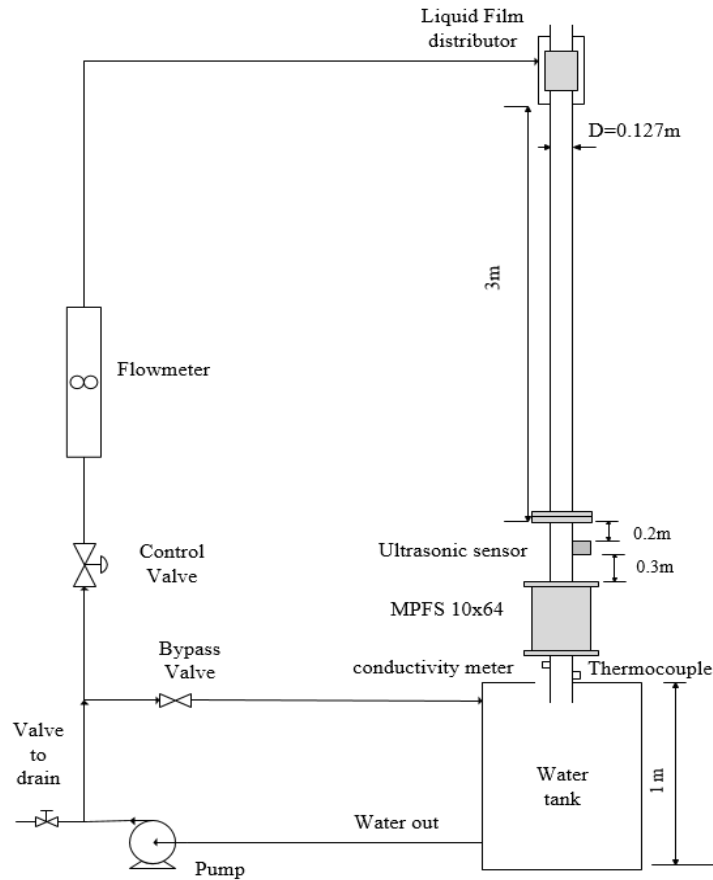
Figure 10: Schematic Diagram of a falling film annular flow test facility.

The free falling liquid film annular flow test facility (Figure 10) has a vertical test section made of acrylic resin (Perspex™) with a 127 mm internal diameter and a length of 5 m. Water was used as the working fluid and there was no gas flow. The test section was connected to a water storage tank. The water was pumped from the water tank using a centrifugal pump and controlled by a manual control valve and a bypass valve to deliver the desired liquid flow rate through a rotameter. The water flow rate was measured by the rotameter (MBP Industries Ltd) with an accuracy of ±5% of full scale. A liquid distributor at the top of the test section was used to ensure a uniform liquid film around the test section. The experiments were performed at ambient temperature (~20°C) and atmospheric pressure and temperature was measured using a T-type thermocouple during all experiments. The ultrasonic measurements were compared with the measurements of a MPFS which was mounted at the lower end of the test section. The ultrasonic sensor and the MPFS were located at 320 cm (25.2D) and 350 cm (27.6D) from the bottom of liquid distributor respectively. The experiments were conducted at different liquid Reynold numbers (Re_l) ranging from 618 to 1670. $R\,e_l = \rho_l u_{sl} \delta / \mu_l = \rho_l Q_l / \pi D \mu_l$, where $u_{sl} = Q_l / \pi D \delta$, ρ_l is liquid density, u_{sl} is liquid superficial velocity, Q_l is liquid volumetric flowrate, D is pipe internal diameter and μ_l is the dynamic liquid viscosity. The length scale used to calculate the liquid Reynolds number is the mean liquid film thickness.

362

14

363 The Multi Pin Film Sensor (MPFS) operates on measurements of the electrical conductance between two
364 electrodes in contact with the liquid film. The MPFS utilised was based on the design of [43]. This is similar
365 to other conductance measurement techniques that have been used in literature [43, 44] except that it
366 has the capability to record measurements in 10 axial locations instead of only one. The MPFS used has
367 64 measurement locations in the circumferential direction and results from the US system were compared
368 with the MPFS measurement in the same circumferential location.
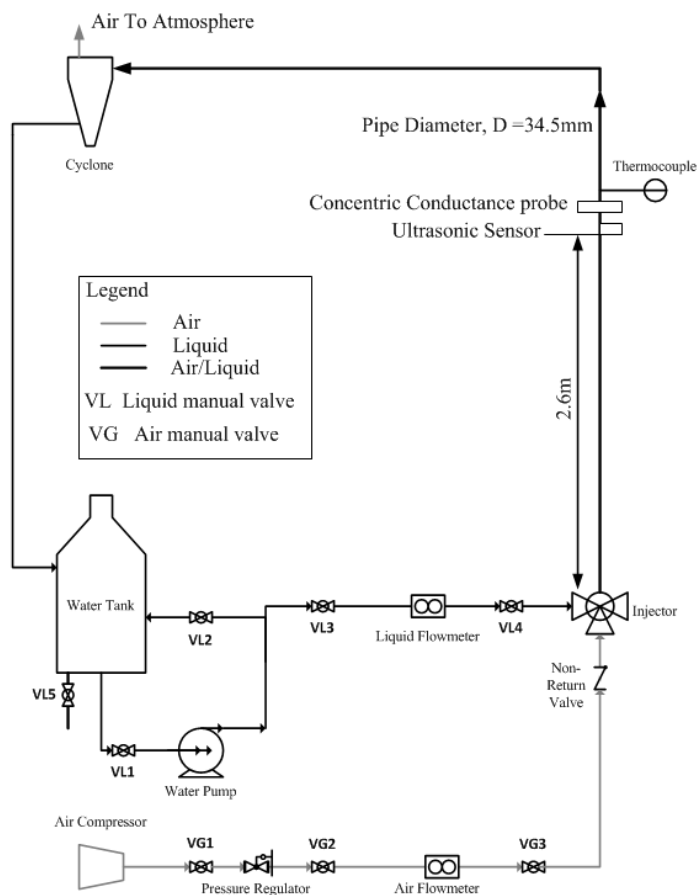
369

370 Figure 11: Schematic Diagram of upward vertical annular flow test facility.

371 The upward vertical annular flow test facility (Figure 11) has a height of 4 m with a 34.5 mm inner
372 diameter and a test section made of acrylic resin (Perspex™). Both liquid and gas flow rate were measured
373 using a calibrated rotameter (MBP Industries Ltd) with an accuracy of ±5%. A conical injector system was
374 used to achieve an annular flow regime similar to the one used by Zhao et al. [45]. The liquid was injected
375 from the side and the gas from the center to create a uniform liquid film around the boundary of the wall.
376 The liquid was injected at four different injection points at the same liquid rate to generate a film around
377 the internal surface of the pipe wall with equal thickness. The airline was equipped with a non-return
378 valve to prevent the flow of water into the gas rotameters. The air/liquid mixture was separated at the
379 top using a cyclone separator. The air was vented to the atmosphere while the water was fed back into
380 the storage tank.

15

381　In these experiments the results of the ultrasonic technique were compared with the results from the
382　concentric conductance probe. The concentric probe operates by relating the film thickness to
383　conductance across two electrodes. The concentric probe works on the same principle as MPFS but was
384　designed to measure the instantaneous film thickness at only four circumferential positions in one axial
385　location. The probe was designed and constructed by Zhao et al. [45] who used it to measure the film
386　thickness in a pipe of diameter 34.5 mm. This probe has also been used by researchers including Azzopardi
387　[46] and Wolf [47] to study multiphase flow. The ultrasonic probe was located in the same circumferential
388　location as one of the 4 concentric probes and separated axially by 70mm from the concentric probe due
389　to flange arrangement. The experiments were conducted at a fixed liquid superficial velocity of 0.089 m/s
390　and different gas superficial velocities ranging from 17.83 to 35.66 m/s.

391　The MPFS and the concentric probe were all calibrated using the same method. This involved inserting
392　different known diameters of non-conducting solid rods (PVC) inside the sensor in which the remaining
393　annulus was filled with water. The water simulates a film of known thickness that can be related to the
394　measured probe output voltage. These rods were machined with high precision to have a uniform
395　diameter. The calibration was repeated three times to ensure the annulus gap represented the expected
396　film thickness. The rod was centered at the bottom using a base block and at the top using a guide. The
397　calibration curves for the concentric probe is shown in Figure 12.
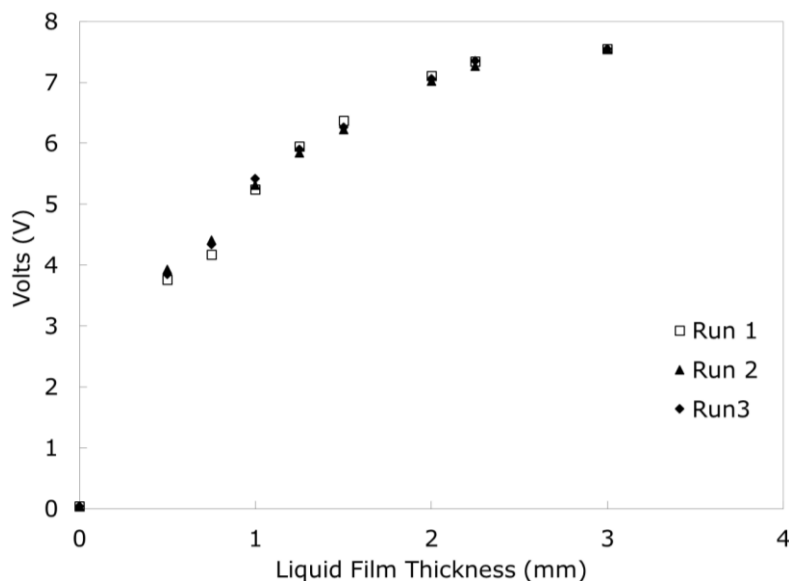
398

399　Figure 12: Calibration curve of the concentric probe. The plot shows the voltage measurements for three
400　repetitions.

401

402

403

404

16

## 4. Experiment Results and Discussion:

5.1 Static Measurements

Figures 13 to 15 show the comparisons of the mean film thicknesses of silicone oil and water obtained by the ultrasonic methods and theoretical calculations (Equation 4) in a static fluid system. Figure 13 and 14 both show results from experiments in silicone oil but the range of film thicknesses is much lower in Figure 14 (0.1 – 0.5 mm), to demonstrate the capabilities of ultrasonic techniques at thinner film thicknesses. For all experiments, the measurements were repeated three times to understand variability and at a temperature of $20^{o}C \pm 0.2^{o}C$. The maximum standard deviation error of the mean at each measurement point between repeated tests was 0.03 mm for both fluids. The TOF method was used for film thicknesses greater than 0.5 mm. Both frequency and baseline removal methods were used for film thicknesses less than 0.5 mm. The standard deviation error was calculated by dividing the standard deviation by the square root of number of repeated points.
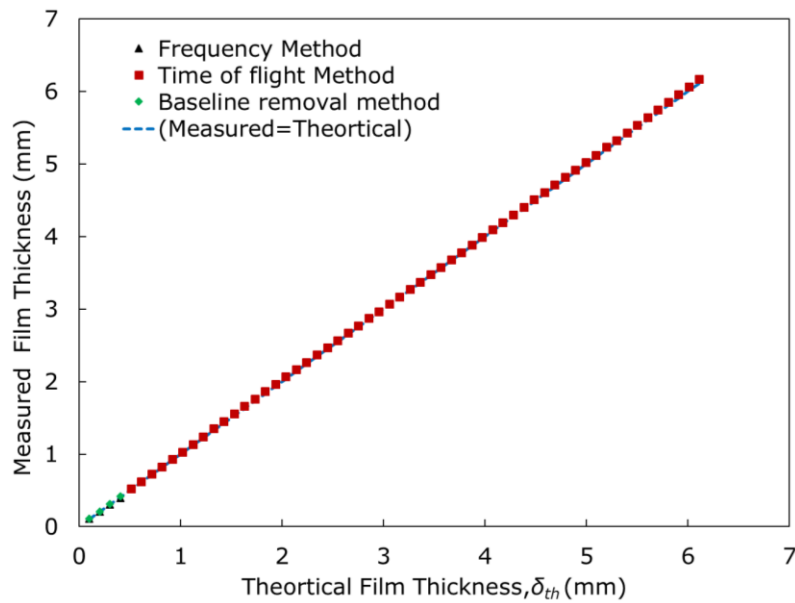
Figure 13: Ultrasonic pulse echo validation results for different processing methods against theoretical calculations (Equation 1) using silicone oil with maximum standard deviation error of 0.03 mm.

17
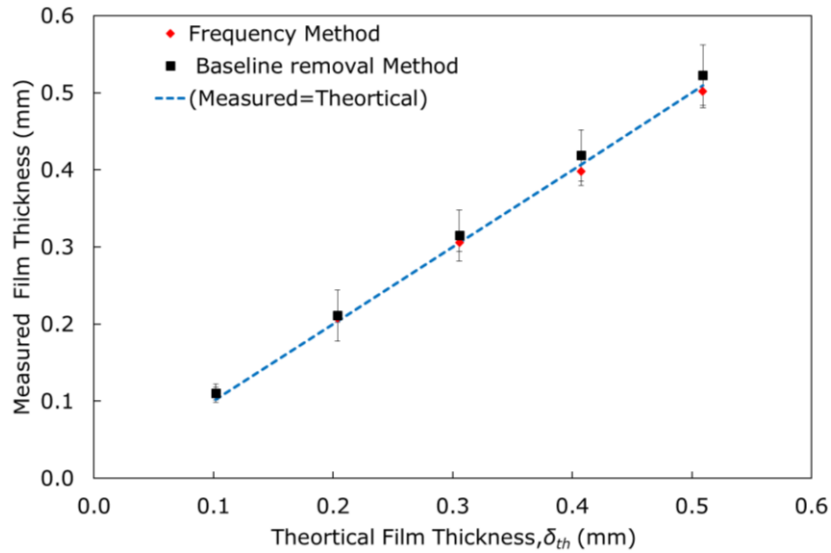
Figure 14: Ultrasonic pulse echo validation results in silicone oil for the frequency domain and baseline removal methods. These are compared to theoretical calculations (Equation 4) based on the volume of fluid added.

From Figures 13 and 14, the ultrasonic technique shows good agreement with the theoretical value for the film thickness calculated using the known volume of silicone oil added and equation 2. The temperature of the silicone oil was recorded and its speed of sound calculate using equation 5. The film thickness measurements between 0.1 mm and 0.5 mm were calculated using the frequency domain and baseline removal methods whereas the larger film thicknesses were calculated using the TOF method.

The static results for water are shown in Figure 15. The TOF method was used to calculate these film thicknesses. The temperature of the water was recorded and equation 6 was used to calculate its speed of sound. Equation 2 was then used to calculate the film thickness which was compared to the theoretical value calculated using the known volume of fluid added and the dimensions of the cylindrical test section. The measured values in Figure 15 for thinner films (2mm and 3mm) are slightly deviated from the calculated value by a maximum relative deviation of 2% due to potential errors in fluid volume, and the speed of sound and temperature measurement accuracy in laboratory conditions. However, it should be noted that there is a better agreement when the film thickness increases. This is due to the improved accuracy of the volume measurements of the liquid, at higher volumes. In general, the ultrasonic results show good agreement with values obtained theoretically.
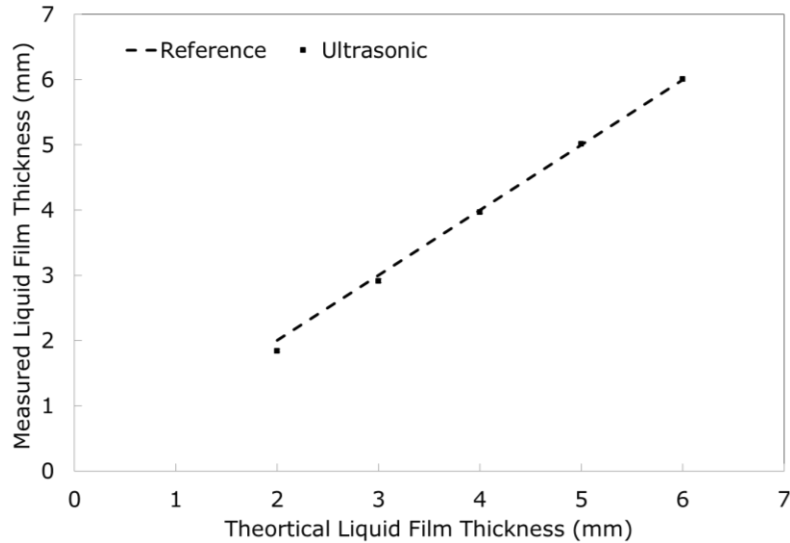
Figure 15: Ultrasonic pulse echo validation results for the time of flight method against theoretical calculations using water.

5.1.1 Effect of Inclination Angle on Ultrasonic Measurement:

As discussed, the received ultrasonic reflections are affected by the angle of the incident waves, which was highlighted as a challenge by Serizawa et al. [21]. Therefore, the effects of the incident wave angle (inclination) was investigated up to 4 degrees. This angle was the upper limit as the liquid was completely removed from the sensor above 4 degrees. These experiments were performed using the rectangular test rig at a 6mm liquid film thickness and a 1 MHz transducer. The detection of the reflected signal from the liquid film/air interface depends on the transducer diameter according to Serizawa et al. [21] and all transducers used in this work had the same diameter of 8mm. Figure 16 shows that the amplitude of the reflected signal decreased as the inclination angle increased, this is because a proportion of the reflected signal is not received by the transducer due to reflecting from a non-perpendicular interface. It was also observed that as the inclination angle increased, the measured time of flight reduced affecting the film thickness measurements. This is in agreement with the observations of Serizawa et al. [21] who used an inclined solid surface placed in water to simulate the reflection interface. Annular flow generally features a base film and the presence of disturbance waves. The amplitude and frequency of these disturbance waves increases as either the gas velocity or volume of water increases [9]. We believe the effects of inclination angle on reflected ultrasonic signals will therefore be less when there are less or smaller disturbance waves which is often the case when the films are thinner and the flow less turbulent.

19

460
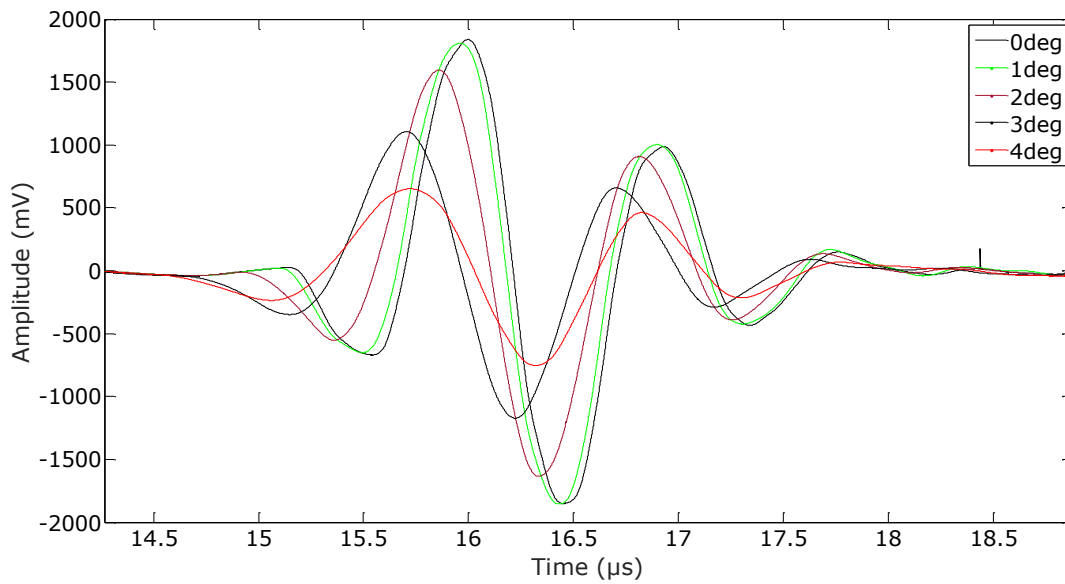
Figure 16: Effects of inclination angle on the received ultrasonic signal.

5.2 Dynamic Measurements

5.2.1 Falling films

Figures 17 and 18 show the instantaneous measurement of the liquid film thickness at liquid Reynolds number 618 using ultrasonic and Multi Pin Film Sensor (MPFS) techniques for a falling film annular flow experiment. There was a vertical spatial separation of 300 mm between the two sensors. The measurement techniques show a good agreement with film thicknesses varying between 0.5 and 2.5 mm.
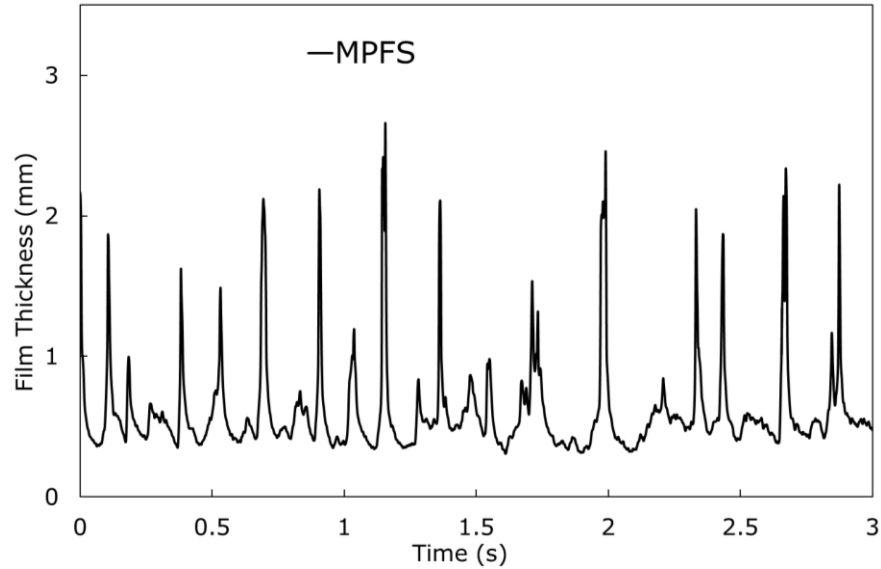

468
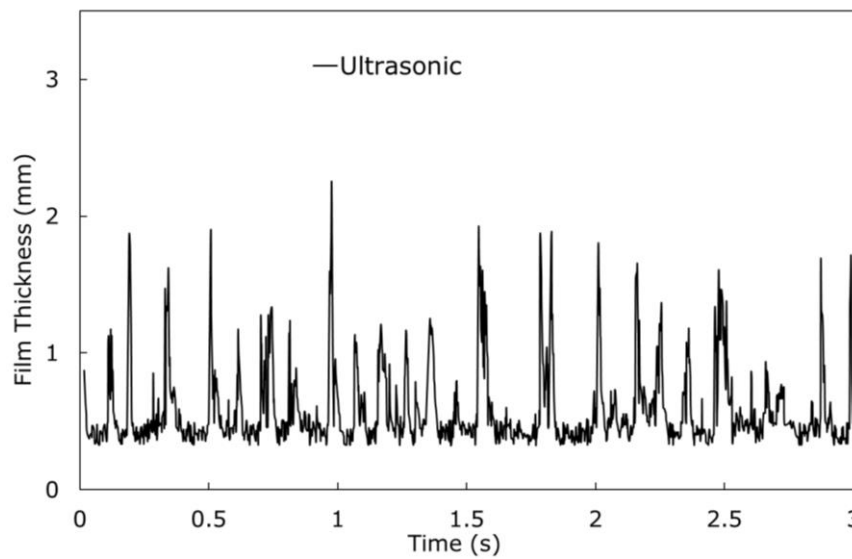
Figure 17: Instantaneous variation of the film thickness using Ultrasonic technique at liquid Reynolds number 618.

471

Figure 18: Instantaneous variation of the film thickness using MPFS at liquid Reynolds number 618.

The frequency of the surface waves in the time series film thickness measurements were calculated using a Power Spectral Density (PSD) for both measurement data sets. The Power Spectral Density (PSD) was obtained using Welch's method within MATLAB. In the Welch's method, the time series signal is divided into small overlapping segments where spectrum analysis using a FFT is computed for each segment before the average spectral estimate for all segments is obtained. In the current analysis, the length of each segment is 500 data points with a 50% overlap between them. The power spectral density of both techniques for different Reynolds number ranged from 618 to 1670 and are shown in Figure 19. Both techniques were able to measure the frequency of the variation in film thickness and showed good agreement with each other. The film thickness exhibits a frequency ranging from 5 Hz to 8 Hz and generally increased with higher liquid Reynolds number.

484
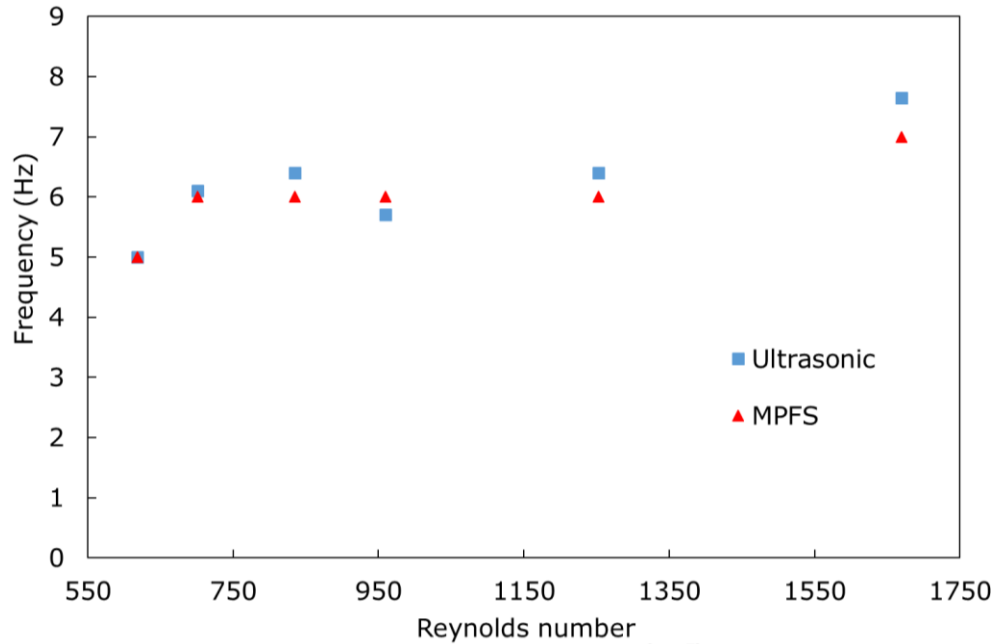
Figure 19: Power Spectral Density (PSD) of the film thickness measurements using MPFS and ultrasonic
techniques at different liquid Reynolds numbers.

Applying the frequency domain method in wavy films is challenging due to moving surfaces and results in many spectral peaks requiring significant post processing and leading to unreliable results as indicated in Figure 20. Further development is required to enhance the capabilities of the frequency domain method to operate on wavy films. The data obtained by the frequency domain method was not used in the current comparisons between the ultrasonic technique and the MPFS. Instead, the baseline removal and time of flight methods were used for calculating the instantaneous film thicknesses.


493
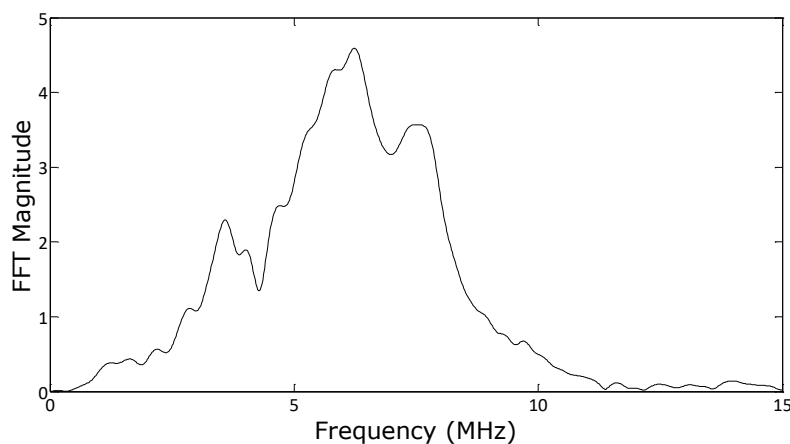
Figure 20: Spectrum Wavy Signal results after applying frequency method on a dynamic wavy film.

In terms of the mean film thickness, the data obtained by the ultrasonic measurements showed good agreement with the Multi Pin Film Sensor (MPFS) with a relative deviation less than ±5% between them.

497   Figure 21 shows the comparison of mean liquid film thickness measurements between the MPFS and the
498   ultrasonic measurements at different liquid Reynolds numbers. Both techniques show the expected trend
499   where the measured film thickness increased as the liquid Reynolds number increased. The results in
500   Figure 21 are consistent with those of Karapantios et al. [48] and Salazar and Marschall [49] which show
501   that an increase in liquid Reynolds number increases the mean film thickness in falling film systems. The
502   liquid Reynolds number is proportional to the volumetric flow rate. Therefore an increase in Re_l results
503   in a larger volume of water in the pipe and a larger mean film thickness. The results in Figure 21 also
504   indicate two regions of different gradients, the first below a liqud Reynolds number of 1000 and second
505   above it. This is most likely the result of a linear thin film transitioning to a larger wavy film. Interestingly
506   the largest difference between the results from ultrasonic and MPFS measurments were at a liquid
507   Reynolds value of 1000 where this transition occurs. Here we believe the MPFS is showing the correct
508   value and there is an error with reading from the ultrasonic sensor caused by the transition from linear
509   thin film flow to wavy film flow.
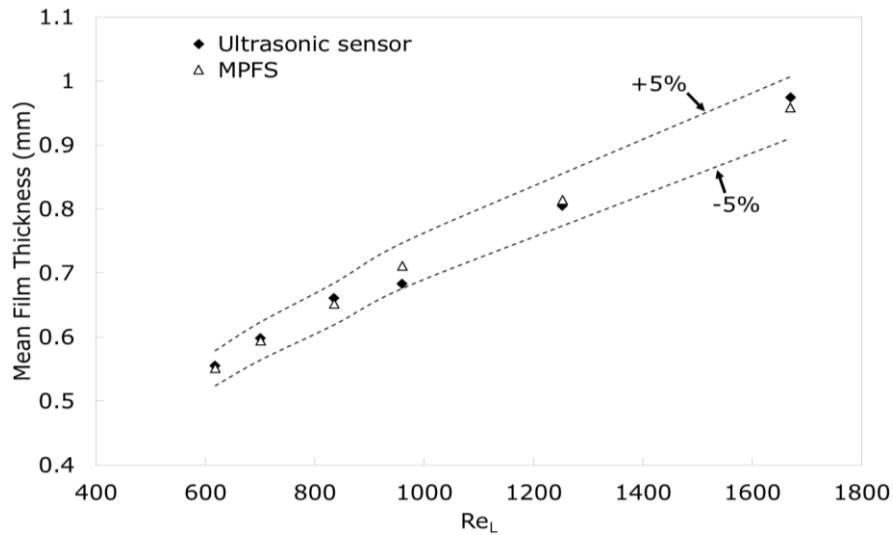
510

511   Figure 21: Mean film thickness between Ultrasonic and MPFS using water with a relative deviation less
512   than ±5% between them.

513 *5.2.2 Upward annular flow*

514   In the upward vertical annular flow experiments, the time series measurements of film thicknesses
515   calculated by the ultrasonic technique showed similar trends to that measured by the concentric
516   conductance probe for the same experimental parameters (Figures 22 and 23). In these experiments there
517   was an axial spatial separation of 70 mm between the two sensors. The film thickness measurements
518   recorded using the ultrasonic technique were calculated using the baseline removal and TOF methods.
519   This was performed to check the capability of baseline removal method for measuring film thicknesses
520   less than 0.5 mm on a flowing test facility.

521   The power spectral density was used to calculate the frequency of the surface waves for both techniques
522   at a liquid superficial velocity of 0.089 m/s and different gas superficial velocities ranging from 17.83 to

523   35.66 m/s (Figure 24). Both techniques were able to measure the variation of the film thickness frequency

524   and agreed with each other. The frequency of the variation in film thickness increases with increasing gas

525   superficial velocities from 7 Hz to 18 Hz.
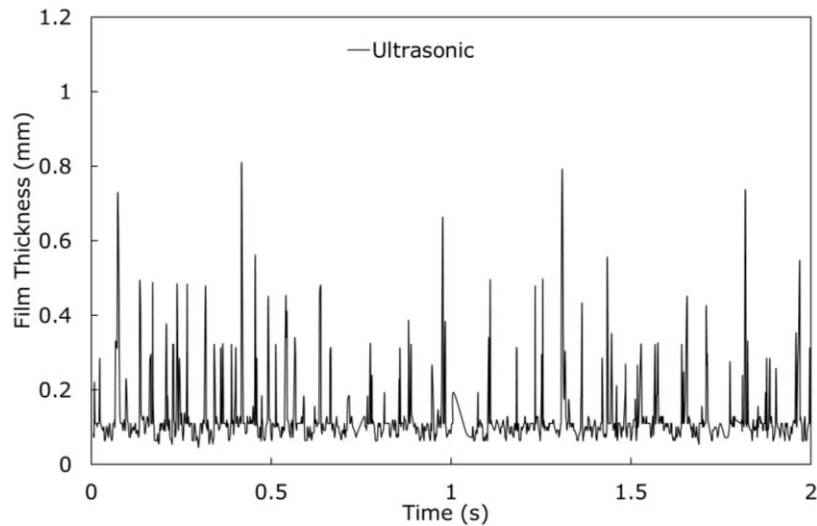

526

527   Figure 22: Instantaneous variation of the film thickness using the ultrasonic technique at water and gas

528   superficial velocities of 0.089 m/s and 35.66 m/s respectively.

529
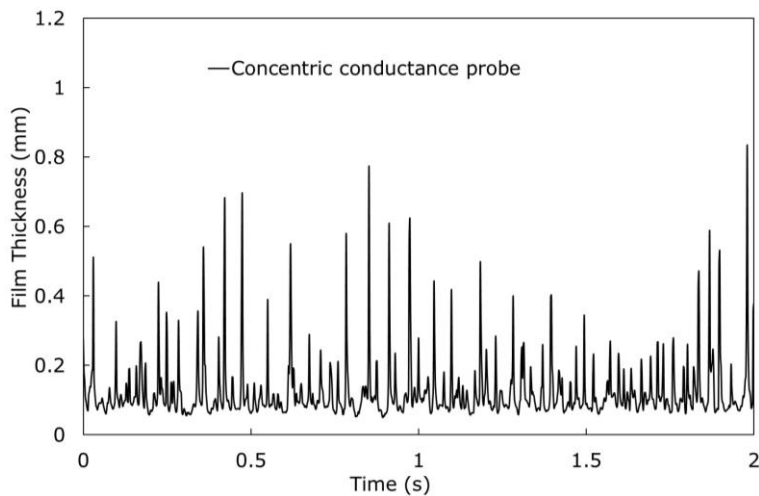
530

531   Figure 23: Instantaneous variation of the film thickness using the concentric conductance probe at water

532   and gas superficial velocities of 0.089 m/s and 35.66 m/s respectively.

533
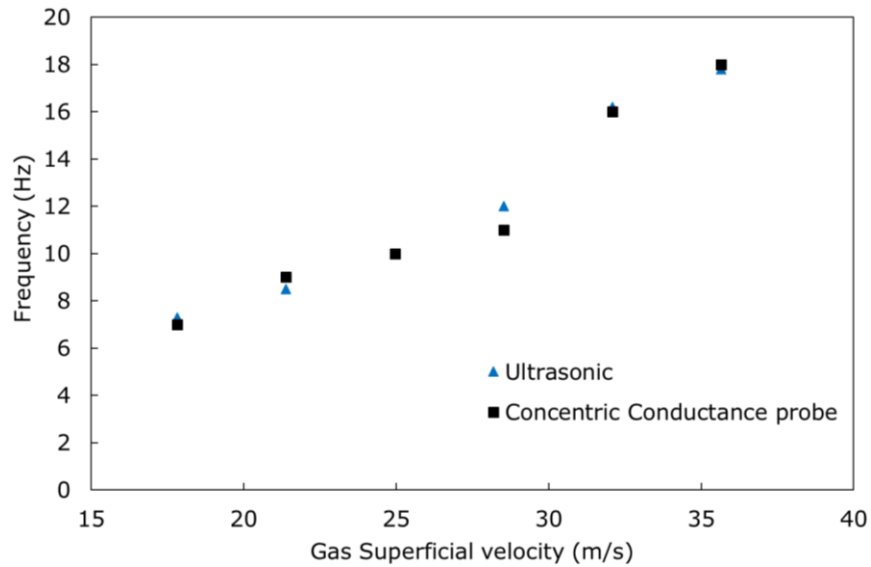
Figure 24: Power Spectral Density (PSD) of the film thickness measurements using the concentric probe
and ultrasonic technique at different gas superficial velocities and water superficial velocity of 0.089
m/s.

The results in Figure 24 indicate that an increase in gas superficial velocity results in an increase in wave
frequency. When the gas and liquid meet at the inlet section the liquid phase is broken down into high
frequency, low amplitude waves due to the shearing of the gas phase. These waves have irregular
velocities and will coalesce with other low amplitude waves as the flow develops [9]. Increasing gas
flowrate increases the interfacial shear and the frequency and velocity of these small waves resulting in
a higher degree of coalescence and the formation of a higher frequency of disturbance waves. These
results are consistent with the the work of Chu and Dukler [50], Azzopardi [46] and Vasques et al. [9].
The ultrasonic technique and concentric conductance probe technique also showed excellent agreement
in term of the mean film thickness measurement with a relative deviation less than ±5% between them.
Both techniques showed the expected trend where the measured film thickness decreased as the gas
superficial velocity increased at fixed liquid superficial velocity (Figure 25).

550
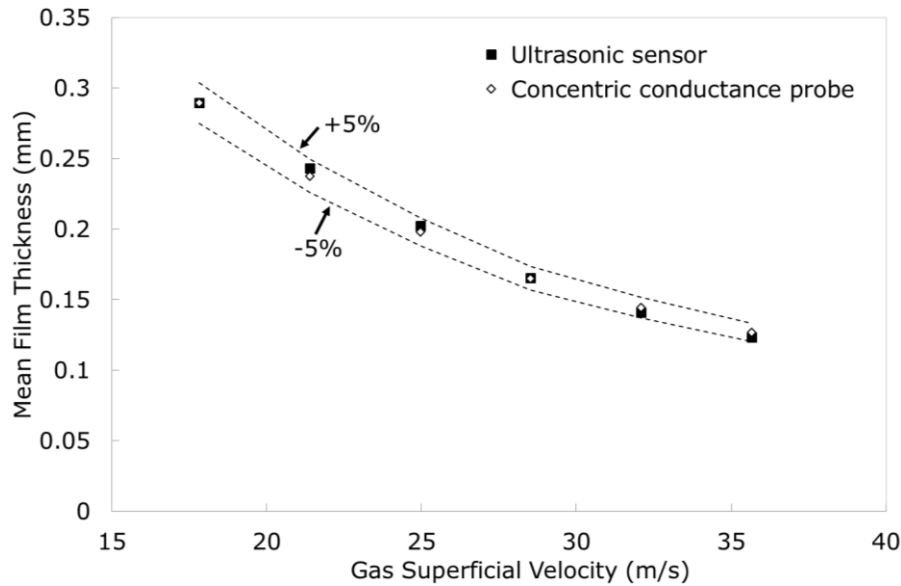
Figure 25: Mean film thicknesses measured using the ultrasonic and concentric conductance techniques at water superficial velocity of 0.089 m/s with a relative deviation less than ±5% between them.

Both static and dynamic measurements show the capabilities of the ultrasonic technique for measuring thin film thicknesses using different signal processing methods. The results also highlights the capability of the baseline removal method for measuring the film thickness when the reflected signals were overlapped in time. Increasing the data acquisition rate will improve the temporal resolution of measured film thicknesses whilst enabling a more accurate calculation of the average film thickness. More data points would also enable characteristics of the instantaneous liquid film to be studied in greater detail in the flowing test facilities. Figure 25 shows that an increase in gas superficial velocity reduces the mean film thickness which again is caused by the increase in interfacial shear and consistent with the results reported by Chu and Dukler [50], Belt et al. [17] and Vasques et al. [9].

5. Conclusion:

In this work, an ultrasonic measurement technique was implemented to measure dynamic film thicknesses between 0.1 mm and 6 mm in liquid-gas systems for silicone oil and water. The ultrasonic measurements were evaluated in static and dynamic environments. It is demonstrated that ultrasonic techniques have the capability to measure the instantaneous liquid film thickness in conducting and non-conducting mediums. The results obtained were in good agreement with theoretical predictions and simultaneous measurements from established sensing technologies (MPFS and concentric probe). For the experimental work in static systems errors due to the temperature dependence of the speed of sound, fluid volume and geometry did not appear to influence the results significantly. The experimental results for instantaneous and mean film thickness in upwards and downwards annular flow showed good agreement between the ultrasonic and conductance sensors with results consistent to those reported in the literature.

574 The baseline removal method of Park et al. [41] was used as the signal processing method when the
575 ultrasonic reflected signals were overlapped in the time domain. This method showed good agreement
576 with an existing frequency domain method, yet requires less computational processing and is simpler to
577 implement. Interestingly the greatest difference between the ultrasonic and established measurement
578 results occurred where changes in the flow behaviour were observed.

579 This work demonstrates the potential of ultrasonic pulse echo techniques for measuring the film thickness
580 in annular flow using a variety of signal processing methods. However challenges still remain when the
581 liquid gas interface experiences large waves due to the angle the incident ultrasonic waves are reflected.

Acknowledgements

6. References:

587 [1] Hewitt, G. F. & Hall-Taylor, N. Annular two-phase flow, Pergamon,1 970.

588 [2] Azzopardi, B.J., Gas-Liquid Flows, Begell house, New York. 2006.

589 [3] Azzopardi, B. J., Drops in annular two-phase flow.   International Journal of Multiphase Flow, 23,
590 Supplement, 1-53, 1997.

591 [4] Thwaites, G. R., Kulov, N. N. & Nedderman, R. M. Liquid film properties in two-phase annular flow.
592 Chemical Engineering Science, 31, 481-486, 1976.

593 [5] Tibirica, C. B., Do Nascimento, F. J. & Ribatski, G. Film thickness measurement techniques applied to
594 micro-scale two-phase flow systems. Experimental Thermal and Fluid Science, 34, 463-473, 2010.

595 [6] Clark, W. W., Liquid film thickness measurement. 14, 74, 2002.

596 [7] Berna, C., Escriva, A., Munoz-Cobo, J. L. & Herranz. Review of droplet entrainment in annular flow:
597 Characterization of the entrained droplets. Progress in Nuclear Energy, 79, 64-86. 2015.

598 [8] Ghosh, S., Mandal, T. K., Das, G. & Das, P. K. Review of oil water core annular flow. Renewable and
599 Sustainable Energy Reviews, 13, 1957-1965. 2009.

600 [9] Vasques, J., Cherdansev, A., Cherdanstev, M., Isaenkov, S. & Hann, D. (2018). Comparison of
601 disturbance wave parameters with flow orientation in vertical annular gas-liquid flows in a small pipe.
602 Experimental Thermal and Fluid Science, 97, 484-501.

603 [10] Zadrazil, I., Matar, O. K. & Markides, C. N. An experimental characterisation of downward gas-liquid
604 annular flow by laser-induced fluoroscence: Flow regimes and film statistics. International Journal of
605 Multiphase Flow, 60, 87-102. 2014.

606   [11] Pham, S. H. & Kunugi, T. Annular flow in rod-bundle: Effect of spacer on disturbance waves. Flow
607   Measurment and Instrumentation, 50, 280-288. 2016.

608   [12] Yu, S. C. M., Tso, C. P. & Liew, R., Analysis of thin film thickness determination in two-phase flow
609   using a multifiber optical sensor. Applied Mathematical Modelling, 20, 540-548, 1996.

610   [13] Pan, L. M., He, H., Ju, P., Hibiki, T. & Ishii, M. Experimental study and modeling of disturbance wave
611   height of vertical annular flow. International Journal of Heat and Mass Transfer, 89, 165-175. 2015.

612   [14] Wang, C., Zhao, N., Fend, Y., Sun, H. & Fang, L. Interfacia wave velocity of vertical gas-liquid annular
613   flow at different system pressures. Experimental Thermal and Fluid Science, 92, 20-32. 2018.

614   [15] Kunugi, T. Summary: Study of wavy interface behavior and droplet entrainment of annular two-
615   phase flow in rod bundle geometry with spacers. Nuclear Engineering and Design, 336, 45-53. 2018.

616   [16] Kang, H. C. & Kim, M. H., The development of a flush-wire probe and calibration method for
617   measuring liquid-film thickness. International Journal of Multiphase Flow, 18, 423-437,1992.

618   [17] Belt, R. J., Van't Westende, J. M. C., Prasser, H. M. & Portela, L. M. 2010. Time and spatially resolved
619   measurements of interfacial waves in vertical annular flow. International Journal of Multiphase Flow, 36,
620   570-587.

621   [18] Chun, J. R. P. M.-H. 1984. Liquid Film Thickness Measurement by An Ultrasonic Pulse Echo Method.
622   Korean Nuclear Society, 17.

623   [19] Ng, T. W., Narain, A. & Kivisalu, M. T., Fluorescence and Fiber-Optics Based Real-Time Thickness
624   Sensor for Dynamic Liquid Films. Journal of Heat Transfer, 132, 031603-031603, 2009.

625   [20] Lu, Q., Suryanarayana, N. V. & Christodoulu, C. 1993. Film Thickness Measurement with an
626   Ultrasonic Transducer. Experimental Thermal and Fluid Science, 7, 354-361.

627   [21] Serizawa, A., Nagane, K., Kamei, T., Takahashi, O. & Kawara, Z.. Non-Intrusive Measurement Of
628   Dynamic Behavior Of A Liquid Film Flow. Proceedings of the German-Japanese Symposium on Multi-
629   Phase Flow, 51-51,1994.

630   [22] Chen, Z. Q., Hermanson, J. C., Shear, M. A. & Pedersen, P. C. Ultrasonic monitoring of interfacial
631   motion of condensing and non-condensing liquid films. Flow Measurement and Instrumentation, 16,
632   353-364, 2005.

633   [23] Wada, S., Kikura, H. & Aritomi, M. 2006. Pattern recognition and signal processing of ultrasonic
634   echo signal on two-phase flow. Flow Measurement and Instrumentation, 17, 207-224.

635   [24] Masala, T., Harvel, G. & Chang, J. S. 2007. Separated two-phase flow regime parameter
636   measurement by a high speed ultrasonic pulse-echo system. Rev Sci Instrum, 78, 114901.

637   [25] Murai, Y., Tasaka, Y., Nambu, Y., Takeda, Y. & Gonzalez A, S. R. 2010. Ultrasonic detection of moving
638   interfaces in gas–liquid two-phase flow. Flow Measurement and Instrumentation, 21, 356-366.

639 [26] Baba Musa, A. & Hoi, Y. 2016. Non-invasive classification of gas–liquid two-phase horizontal flow
640 regimes using an ultrasonic Doppler sensor and a neural network. Measurement Science and
641 Technology, 27, 084002.

642 [27] Fachun, L., Hongfeng, Z., Hao, Y. & Yuan, S. 2016. Gas–liquid two-phase flow pattern identification
643 by ultrasonic echoes reflected from the inner wall of a pipe. Measurement Science and Technology, 27,
644 035304.

645 [28] Watson N. J. Ultrasound Tomography. In: M WANG, ed., Industrial Tomography: Systems and
646 applications Woodhead Publishing. 235-257, 2015.

647 [29] Dwyer-Joyce, R.S., Drinkwater, B.W. and Donohoe, C.J. (2003) The measurement of lubricant-film
648 thickness using ultrasound. Proceedings of the Royal Society Series A: Mathematical Physical and
649 Engineering Sciences, 459 (2032). pp. 957-976.

650 [30] Zhang, J., Drinkwater, B. W. & Dwyer-Joyce, R. S. Calibration of the Ultrasonic Lubricant-film
651 thickness measurement technique. Measurement Science and Technology, 16, 1784-1791. 2005.

652 [31] Challis, R. E., Alper, T., Holmes, A. K. & Cocker, R. P. Near-plane-wave acoustic propagation
653 measurements in thin layers of adhesive polymer. Measurement Science and Technology, 2, 59-68.
654 1991.

655 [32] Wang, L., Xie, B. & Rokhlin, S. I. Determination of embedded layer properties using adaptive time-
656 frequency domain analysis. The Journal of the Acoustical Society of America, 111. 2002.

657 [33] Dwyer-Joyce, R. S., Harper, P., Pritchard, J. and Drinkwater, B.W. Oil film measurement in
658 polytetrafluoroethylene-faced thrust pad bearings for hydrogenerator applications. Proceedings of the
659 Institution of Mechanical Engineers, Part A: Journal of Power and Energy, 220, 6. 2006.

660 [34] Drinkwater, B. W., Zhang, J., Kirk, K. J., Elgoyhen, J. & Dwyer-Joyce, R. S. Ultrasonic measurement of
661 rolling bearing lubrication using piezoelectric thin films. Jounral of Tribology, 131, 2009.

662 [35] Dwyer-Joyce, R.S., Reddyhoff, T. and Drinkwater, B. (2004) Operating Limits for Acoustic
663 Measurement of Rolling Bearing Oil Film Thickness. Tribology Transactions, 47, 3, 366-375.

664 [36] Jhang, K., Jang, H., Park. B., Ha, J., Park, I. & Kim, K. Wavelet analysis based deconvolution to
665 improve the resolution of scanning acoustic microscope images for the inspection of thin die layer in
666 semiconductor. NDT&E International, 35, 549-557. 2002.

667 [37] Kinra, V. K., Jaminet, P. T., Zhu, C. & Iyer, V. R. Simultaneous measurement of the acoustical
668 properties of a thin-layered medium: The Inverse problem. The Jounral of the Acoustical Society of
669 America, 95. 1994.

670 [37] Jiao, J., Liu, W., Zhang, J., Zhang, Q., He, C. & Wu, B. Time frequency analysis for ultrasonic
671 measurement of liquid-layer thickness. Mechanical systems and signal processing, 35, 69-83.

672 [38] Cowell, D. M. J. & Freear, S. Separation of Overlapping Linear Frequency Modulated (LFM) Signals
673 Using the Fractional Fourier Transform. IEEE Transactions of Ultrasonics, Ferroelectrics, and Frequency
674 Control, 57, 10. 2010.

675 [39] Mor, E., Azoulay. & Aladjem, M. A Matching Pursuit Method for Approximating Overlapping
676 Ultrasonic Echoes. IEEE Transactions of Ultrasonics, Ferroelectrics, and Frequency Control, 57, 9. 2010.

677 [40] Zhang, K., Meng, Q., Geng, T. & Wang, N. Ultrasonic measurments of lubricant film thickness in
678 sliding bearings with overlapped echoes. Tribology International, 88, 89-94, 2015.

679 [41] Park, H. J., Tasaka, Y. & Murai, Y. Ultrasonic pulse echography for bubbles travelling in the proximity
680 of a wall. Measurement Science and Technology, 26. 2015.

681 [42] Bilaniuk N. and Wong G. S. K., Erratum: Speed of sound in pure water as a function of temperature
682 J. Acoust. Soc. Am. 99(5), p 3257,1996.

683 [43] ZANGANA, M. H. S. 2011. Film behaviour of vertical gas-liquid flow in a large diameter pipe. Ph.D.
684 Thesis, University of Nottingham.

685 [44] ZABARAS, G., DUKLER, A. E. & MOALEM-MARON, D. 1986. Vertical upward cocurrent gas-liquid
686 annular flow. AIChE Journal, 32, 829-843.

687 [45] Zhao, Y., Markides, C. N., Matar, O. K. & Hewitt, G. F. 2013. Disturbance wave development in two-
688 phase gas–liquid upwards vertical annular flow. International Journal of Multiphase Flow, 55, 111-129.

689 [46] Azzopardi, B. J. (1986). "Disturbance wave frequencies, velocities and spacing in vertical annular
690 two-phase flow." Nuclear Engineering and Design 92(2): 121-133.

691 [47] WOLF, A. 1995. liquid film structure in annular two-phase flow. Ph.D. Thesis, , University of London,
692 Imperial College.

693 [48] Karapantsios, T. D. and A. J. Karabelas (1995). "Longitudinal characteristics of wavy falling films."
694 International Journal of Multiphase Flow 21(1): 119-127.

695 [49] Salazar, R. P. and E. Marschall (1978). "Time-average local thickness measurement in falling liquid
696 film flow." International Journal of Multiphase Flow 4(4): 405-412.

697 [50] Chu, K. J. and A. E. Dukler (1975). "Statistical characteristics of thin, wavy films III. Structure of the
698 large waves and their resistance to gas flow." AIChE Journal 21(3): 583-593.